U.S. Phase I First-in-human Study of Taletrectinib (DS-6051b/AB-106), a ROS1/TRK Inhibitor, in Patients with Advanced Solid Tumors

Kyriakos P. Papadopoulos[1], Erkut Borazanci[2], Alice T. Shaw[3,4], Ryohei Katayama[5], Yuki Shimizu[5], Viola W. Zhu[6], Thomas Yang Sun[7], Heather A. Wakelee[7], Russell Madison[8], Alexa B. Schrock[8], Giorgio Senaldi[9], Naoki Nakao[10], Hiroyuki Hanzawa[10], Masaya Tachibana[11], Takeshi Isoyama[11], Kenji Nakamaru[11], Chenhui Deng[12], Meijing Li[13], Frank Fan[13], Qinying Zhao[13], Yanfei Gao[13], Takashi Seto[14], Pasi A. Jänne[15], and Sai-Hong Ignatius Ou[6]

ABSTRACT

Purpose: Taletrectinib (DS-6051b/AB-106) is an oral, tyrosine kinase inhibitor of ROS1 and NTRK with potent preclinical activity against *ROS1* G2032R solvent-front mutation among others. We report the first-in-human U.S. phase I results of taletrectinib.

Patients and Methods: Patients ≥18 years old with neuroendocrine tumors, with tumor-induced pain, or tumors harboring *ROS1*/*NTRK* rearrangements were eligible. Accelerated titration followed by modified continuous reassessment method and escalation with overdose control was used (50–1,200 mg once daily or 400 mg twice daily). Primary objectives were safety/tolerability, and MTD determination. Secondary objectives were food-effect pharmacokinetics and antitumor activity.

Results: A total of 46 patients were enrolled. Steady-state peak concentration (C_{max}) and exposure ($AUC_{0\text{-}8}$) increased dose dependently from 50-mg to 800-mg once-daily doses. The ratio of the geometric mean of $AUC_{0\text{-}24}$ between low-fat-diet-fed/fasted state was 123% (90% confidence interval, 104%–149%). Dose-limiting toxicities (grade 3 transaminases increase) occurred in two patients (1,200-mg once-daily dose). MTD was 800 mg once daily. Most common treatment-related adverse events were nausea (47.8%), diarrhea (43.5%), and vomiting (32.6%). Pain score reductions were observed in the 800-mg once-daily dose cohort. Confirmed objective response rate was 33.3% among the six patients with RECIST-evaluable crizotinib-refractory *ROS1*$^+$ NSCLC. One patient with *TPM3-NTRK1* differentiated thyroid cancer achieving a confirmed partial response of 27 months at data cutoff. We identified a cabozantinib-sensitive *ROS1* L2086F as an acquired taletrectinib-resistance mutation.

Conclusions: Taletrectinib has manageable toxicities at the MTD of 800 mg daily. Preliminary efficacy was observed in patients with crizotinib-refractory *ROS1*$^+$ NSCLC.

Introduction

Receptor tyrosine kinase fusions are actionable driver alterations in solid malignancies (1). Tyrosine kinase inhibitors (TKIs) targeting these fusions such as crizotinib and entrectinib for *ROS1* fusion–positive non–small cell lung cancer (NSCLC) and larotrectinib and entrectinib for TRK fusion–positive malignancies have been approved for clinical use (2–5). Resistance to these TKIs invariably develops and usually involves second site mutations such as gatekeeper mutation, xDFG motif mutations, and solvent-front mutation (1). Development of next-generation TKIs that can inhibit these acquired mutations is needed.

Furthermore, TrkB (*NTRK2*) signaling pathway is considered to be involved in the proliferation, tumorigenesis, and invasive nature of neuroendocrine tumors (NETs; ref. 6). In addition, ligand to the TRK receptors kinase such as nerve growth factor (NGF) which is a ligand to TrkA is involved in pain sensation and strategy to block NTRK pathway has been investigated for pain control TrkA (7).

Taletrectinib (DS6051b/AB-106) is a highly selective type I ROS1/NTRK inhibitor. Taletrectinib demonstrates an enzymatic inhibition concentration at 50% (IC_{50}) against ROS1, NTRK1, NTRK2, and NTRK3 of 0.207 nmol/L, 0.622 nmol/L, 2.28 nmol/L, and 0.980 nmol/L, respectively (8). In addition, it has potent growth inhibitory activity against both *ROS1* L2026M gatekeeper mutation and *ROS1* G2032R solvent-front mutation (growth inhibition at 50% $GI_{50} = 4$ nmol/L against ETV6-ROS1 wild-type (WT); $GI_{50} = 14$ nmol/L against ETV6-ROS1 L2026M; $GI_{50} = 64$ nmol/L against ETV6-ROS1 G2032R; refs. 8, 9). *In silico* docking study indicated while taletrectinib

[1]South Texas Accelerated Research Therapeutics, San Antonio, Texas. [2]HonorHealth and Translational Genomics Research Institute, Scottsdale, Arizona. [3]Novartis Institute of BioMedical Research, Cambridge, Massachusetts. [4]Massachusetts General Hospital, Harvard Medical School, Boston, Massachusetts. [5]Cancer Chemotherapy Center, Japanese Foundation for Cancer Research, Tokyo, Japan. [6]Chao Family Comprehensive Cancer Center, University of California, Irvine School of Medicine, Orange, California. [7]Department of Medicine, Division of Oncology, Stanford University, Stanford Cancer Institute, Stanford, California. [8]Foundation Medicine Inc, Cambridge, Massachusetts. [9]Daiichi Sankyo, Inc., Basking Ridge, New Jersey. [10]Daiichi Sankyo RD Novare Co., Ltd, Tokyo, Japan. [11]Daiichi Sankyo, Co., Ltd, Tokyo, Japan. [12]Linking Truth Technology Co, Ltd, Beijing, China. [13]AnHeart Therapeutics (Hangzhou) Company Ltd, Hangzhou, Zhejiang province, China. [14]Department of Thoracic Oncology, National Hospital Organization Kyushu Cancer Center, Fukuoka, Japan. [15]Dana-Faber Cancer Institute, Harvard Medical School, Boston, Massachusetts.

Note: Supplementary data for this article are available at Clinical Cancer Research Online (http://clincancerres.aacrjournals.org/).

Prior presentation: Presented at the 2018 annual meeting of the American Society of Clinical Oncology (J Clin Oncol 36:15s, 2018 (suppl; abstr 2514).

Corresponding Author: Sai-Hong Ignatius Ou, University of California Irvine School of Medicine, Department of Medicine, 200 South Manchester Avenue, Suite 400, Orange, CA 92868. Phone: 714-456-5153; Fax: 714-456-2242; E-mail: siou@hs.uci.edu

Clin Cancer Res 2020;26:4785–94

doi: 10.1158/1078-0432.CCR-20-1630

Translational Relevance

Receptor tyrosine kinase *ROS1* fusion is an actionable driver mutation in solid malignancy. Crizotinib and entrectinib are two ROS1 tyrosine kinase inhibitors approved by the FDA to treat ROS1 fusion–positive non–small cell lung cancer. Resistance to ROS1 TKI invariably occurs and the most common on-target resistance mechanism is the emergence of an acquired solvent-front mutation, *ROS1* G2032R. Taletrectinib is a next-generation ROS1/NTRK inhibitor that can inhibit ROS1 G2032R potently *in vitro*. In this U.S. phase I study, taletrectinib was well tolerated and the MTD was 800 mg once daily. Preliminary activity of taletrectinib in crizotinib-refractory *ROS1*$^{+}$ NSCLC and TRK TKI-naive *NTRK1* fusion–positive malignancy was observed. We identified a novel acquired resistance *ROS1* mutation, *ROS1* L2086F, as an on-target resistance mechanism to taletrectinib that can be inhibited by cabozantinib, a type II ROS1 TKI *in vitro*. A *CD74-ROS1* L2086F NSCLC patient-derived durable clinical benefit with cabozantinib immediately post-taletrectinib.

and crizotinib fits into the WT ROS1 kinase domain (Supplementary Fig. S1A and S1B, respectively), the arginine at position 2032 still allows the binding of taletrectinib into the ROS1 kinase domain (Supplementary Fig. 1C). Arg2032 induces steric hindrance of crizotinib binding to ROS1 kinase domain (Supplementary Fig. S1D). provides steric hindrance to. We conducted a phase I safety and tolerability study of taletrectinib in the United States with an exploratory expansion cohort investigating the preliminary activity of taletrectinib in patients with primary *ROS1* or *NTRK* rearrangement and also patients with NET or patients with cancer pain from tumors.

Patients and Methods

This was a U.S. multicenter, nonrandomized, open-label, multiple-dose, first-in-human study of taletrectinib in patients with metastatic and/or unresectable solid tumors. The trial consisted of three portions: dose escalation, food effect, and an exploratory portion that enrolled patients with *ROS1/NRTK* alterations (determined by the tests performed at the investigators' local institutions or commercial sequencing companies) at the MTD. The study was conducted under the International Conference on Harmonization of Technical Requirements for Registration of Pharmaceuticals for Human Use Guideline for Good Clinical Practice. Written informed consent was obtained from all patients by the investigators and institutional review board of each investigational site approved the study.

The primary objectives for the dose-escalation portion were to assess the safety and tolerability of taletrectinib and to determine the dose-limiting toxicities (DLTs) and the MTD. The primary objective for the food effect portion of the study was to determine the effect of food on the pharmacokinetics (PK) of taletrectinib. Main secondary objective for both portions of the trial was to assess the preliminary objective response rate (ORR). The primary objective of the exploratory cohort was to investigate the preliminary clinical activity of taletrectinib against *ROS1/NTRK1-3* rearranged tumors. Tumor assessments were every three cycles by RECIST 1.1. for the dose escalation and food-effect cohorts and every two cycles for the dose expansion cohort.

Patients with advanced NET were eligible as TrkB (*NTRK2*) signaling pathway is considered to be involved in the proliferation, tumorigenesis, and invasive nature of NET (6). In addition, patients with tumor-induced pain from advanced solid tumors, and patients with *ROS1/NRTK1-3* rearranged tumors were eligible. Other major eligibility criteria included age > 18 years old, ECOG PS of 0-1, at least one extracranial RECIST (1.1) measurable lesion, adequate organ function [platelet count $\geq 100 \times 10^9$/L; hemoglobin ≥9.0 g/dL; absolute neutrophil count $\geq 1.5 \times 10^9$/L; calculated CrCl ≥60 mL/minute or serum creatinine ≤1.5 × upper limited normal (ULN); AST/ALT levels ≤3 × ULN (≤5 × ULN if liver metastases are present) and bilirubin ≤1.5 × ULN]. Major exclusion criteria included untreated and symptomatic central nervous system (CNS) metastases, active HIV, Hepatitis B or C infection, QTcF > 450 ms at baseline, history of myocardial infraction within 6 months of enrollment, or New York class III/IV congestive heart failure.

Initial dose escalation followed the accelerated titration design with single subjects per cohort with a dose increment of 100% from the previous dose to minimize the number of subjects treated at subtherapeutic doses. Accelerated titration design would stop if one grade ≥2 adverse event according to the NCI Common Terminology Criteria for Adverse Events version 4 (NCI-CTCAE, v4) occurred during cycle 1 or one DLT event during cycle 1. Dose escalation would then follow traditional "3 + 3" design guided by the modified continuous reassessment method using a Bayesian logistic regression model and escalation with overdose control (10, 11).

Nonhematologic/nonliver enzymes elevation DLTs are defined as treatment-emergent adverse events (TEAE) ≥grade 3 not attributed to disease or disease-related process. DLTs were also defined as inability to complete at least 75% of the prescribed taletrectinib doses in the first 21 days as a result of nondisease-related ≥grade 2 AE; or a delay of ≥7 days in initiating cycle 2 of therapy because of persistent nondisease-related ≥grade 2 AE. Definitions of hematologic and liver enzymes elevations DLT are listed in Supplementary Table S1.

On the basis of 4 weeks of daily repeated-dose toxicity studies, the severely toxic dose in 10% of rats (STD10 = 100 mg/kg/day or 600 mg/m^2/day) and the highest nonseverely toxic dose (HNSTD = 100 mg/kg/day or 1,200 mg/m^2/day) in monkeys were determined. At this dose level, taletrectinib was generally tolerated and any findings were mainly resolved after a 4-week recovery period. One-tenth of STD10 is 60 mg/m^2 while 1/6 of HNSTD 200 mg/m^2. The 1/10 of STD10 in rats (60 mg/m^2) is not considered a toxic dose in monkeys; therefore, the rat is considered the more sensitive species. Thus, the estimated maximum starting dose for this phase I clinical study would be 60 mg/m^2 (1.62 mg/kg) which is equivalent to a flat dose of 97.2 mg for a 60-kg person or approximately 100 mg. However, as a conservative approach, the starting dose of 50 mg/day is selected for this study based on nonclinical pharmacology study this starting dose still has the potential to demonstrate pharmacologic activity in humans (8).

Taletrectinib was dosed once daily in 21-day cycles. The dose escalation cohorts were 50, 100, 200, 400, 800, and 1,200 mg once daily. A 400-mg twice-daily cohort was added after 800 mg once daily was determined to be MTD. Dose reductions are 400 mg decrements. Standard PK parameters (C_{max}, T_{max}, and AUC) were determined using a noncompartmental analysis approach.

The food effect schema is shown in Supplementary Fig. S2. Patients were assigned to receive a single dose of taletrectinib 400 mg under fasted or fed (low-fat meal) conditions on days -7 and -1, and then received taletrectinib 800 mg once daily (MTD) for a 21-day cycle. Low-fat meal consisted of 400–500 kcal per meal (100–125 kcal from fat, 11–14 grams of fat, and 25% fat composition). For food-effect evaluation, the ANOVA model was performed using log-transformed C_{max} and AUC values.

Exploratory subject-reported pain intensity assessment was performed on patients in the dose-escalation portion at screening and every 7 days of taletrectinib treatment. Prior to taking the daily dose of taletrectinib on those days, pain intensity was measured using a visual analogue scale (0: least possible, 100: worst possible) on the Memorial Pain Assessment Card (12).

AEs were tabulated by event, relationship, and CTCAE grade. Summary statistics were calculated for safety parameters and efficacy parameters. ORR was calculated as the proportion of subjects demonstrating the best overall response of complete response (CR) or partial response (PR). Disease control rate (DCR) was calculated as the proportion of subjects demonstrating the best overall response of CR, PR, or stable disease (SD). Ninety-five percent confidence intervals (95%CI) were calculated on the basis of Wilson method (13).

In vitro inhibition of *ROS1* L2086F

cDNA encoding WT or L2086F-mutated CD74-ROS1 were cloned into pLenti6.3 (Invitrogen) using LR clonase. Each plasmid was transfected into 293FT cells by Fugene HD (Promega). Twenty-one hours after transfection, 300 nmol/L of ROS1 inhibitors (crizotinib, taletrectinib, lorlatinib, or cabozantinib) were treated for 3 hours. Then, the cell lysates were prepared using 1× SDS lysis buffer [1% SDS and 10 % glycerol in 100 mmol/L Tris-HCl (pH7.5)]. Equal amount of proteins was electrophoresed and were immunoblotted with antibodies against phospho-ROS1 (Tyr2274, catalog no. 3078, Cell Signaling Technology), ROS1 (69D6, catalog no. 3266, Cell Signaling Technology), and β-actin (Sigma-Aldrich). All the primary antibody was used 1:1,000 dilution for immunoblot analysis. Taletrectinib, crizotinib, and lorlatinib were synthesized at DaiichiSankyo Co. Ltd. Cabozantinib were purchased from ShangHai Biochempartner. Each compound was dissolved in DMSO for the cell culture experiments.

Statistical calculations

Duration of response (DOR) was calculated as the time from the first observation of response to the date of the first documentation of progressive disease (PD) according to RECIST 1.1 or death due to any cause, whichever occurred first. Time to progression (TTP) was defined as the time from the start of taletrectinib treatment to the date of the first documentation of PD according to RECIST 1.1. Progression-free survival (PFS) time was defined as the time from the start of taletrectinib treatment to the date of the first documentation of PD according to RECIST 1.1 or death due to any cause (whichever occurs first). PFS and TTP were summarized descriptively using the Kaplan–Meier method. Statistical analysis was performed using SAS (version. 9.4).

Results

The trial began on September 24, 2014 and the data cutoff date was March 11, 2019. A total of 46 patients were enrolled (35 patients in the dose-escalation cohort, 11 patents in the food-effect cohort, and eight patients in the dose-expansion ROS1/NTRK cohort; **Table 1**; Supplementary Fig. S3). The majority of the patients were heavily pretreated with 82.6% of the patients having received ≥3 prior treatments. Three patients remained on treatment at the time of data cutoff. There were no patients with RECIST-defined measurable CNS metastasis enrolled.

PK

The plasma concentration of taletrectinib increased in a dose-dependent manner by visual inspection on cycle 1 day 1 (**Fig. 1A**).

Table 1. Patient demographics and baseline characteristics ($N = 46$).

	Dose escalation and expansion ($N = 35$)	Food effect ($N = 11$)	Total ($N = 46$)
Age, years (median range)	62 (27–79)	50 (24–75)	62 (24–79)
≥65 years, *n* (%)	14 (40.0)	4 (36.4)	18 (39.1)
Female, *n* (5)	20 (57.1)	5 (45.5)	25 (54.3)
Race, *n* (%)			
Caucasian	30 (85.7)	11 (100)	41 (89.1)
African-American	2 (5.7)	0	2 (4.3)
Asian	1 (2.9)	0	1 (2.2)
American Indian or Alaska Native	1 (2.9)	0	1 (2.2)
Other	1 (2.9)	0	1 (2.2)
Baseline PS, *n* (%)			
0	11 (31.4)	4 (26.4)	15 (32.6)
1	24 (68.6)	7 (63.6)	31 (67.4)
Cancer type, *n* (%)			
Neuroendocrine	8 (22.9)	4 (36.4)	12 (26.1)
NSCLC	8 (22.9)	0	8 (17.4
Pancreas	6 (17.1)	1 (9.1)	7 (15.2)
Colorectal	3 (8.6)	1 (9.1)	4 (8.7)
Lung NOS	2 (5.8)	0	2 (4.3)
Leiomyosarcoma	1 (2.9)	2 (18.2)	3 (6.5)
Bladder	0	2 (18.2)	2 (4.3)
Others[a]	7 (20.0)	1 (9.1)	8 (17.4)
Known molecular alterations[b]			
ROS1	9 (25.7)	0	9 (19.6)
NTRK	1 (2.9)	2 (18.2)	3 (6.5%)
Other	25 (71.4)	9 (81.8)	34 (73.9)
Number of prior regimens, *n* (%)			
<3	4 (11.4)	4 (36.4)	8 (17.4)
≥3	31 (88.6)	7 (63.6)	38 (82.6)

Abbreviation: NOS, not otherwise specified.
[a]Others: One of each: appendiceal (food effect), breast, desmoid tumor, high-grade serous carcinoma of the fallopian tube, inflammatory myofibroblastic tumor, osteosarcoma, small-bowel carcinoma.
[b]Included mutations and fusions

The steady-state plasma concentration of taletrectinib also increased in a dose-proportional manner (**Fig. 1B**). $AUC_{0\text{-}8}$ and C_{max} increase of taletrectinib at steady state is approximately dose-proportional. T_{max} of taletrectinib is achieved around 4–5 hours postdose. Steady state is achieved on day 8. The geometric mean C_{max} and AUC values as well as median T_{max} values were listed in Supplementary Table S2.

The percentage of the unbound fraction (%fu) of taletrectinib in human plasma was 3.5% and 6.28% at 100 and 1,000 ng/mL, respectively. At 50-, 100-, and 200-mg dose levels, mean plasma concentrations of taletrectinib at steady state (cycle 1 day 8/day 15) were less than 104 ng/mL so %fu of 3.5% was used to calculate free drug concentration. At dose range of 400–1,200 mg (cycle 1 day 15), mean drug plasma concentrations were > 100 and up to 918 ng/mL hence %fu of 6.28% was used to calculate free drug concentrations. At the 200-mg once-daily level, the projected free drug level of taletrectinib is above the IC_{90} against WT ROS1 (3.4 nmol/L). At the 400-mg once-daily level, the projected free drug level of taletrectinib is at the level needed for inhibiting 90% (IC_{90}) against *ROS1* G2032R (28.7 nmol/L). At the 800-mg once-daily level, the projected free drug level is consistently above the IC_{90} level against *ROS1* G2032R (**Fig. 1C**).

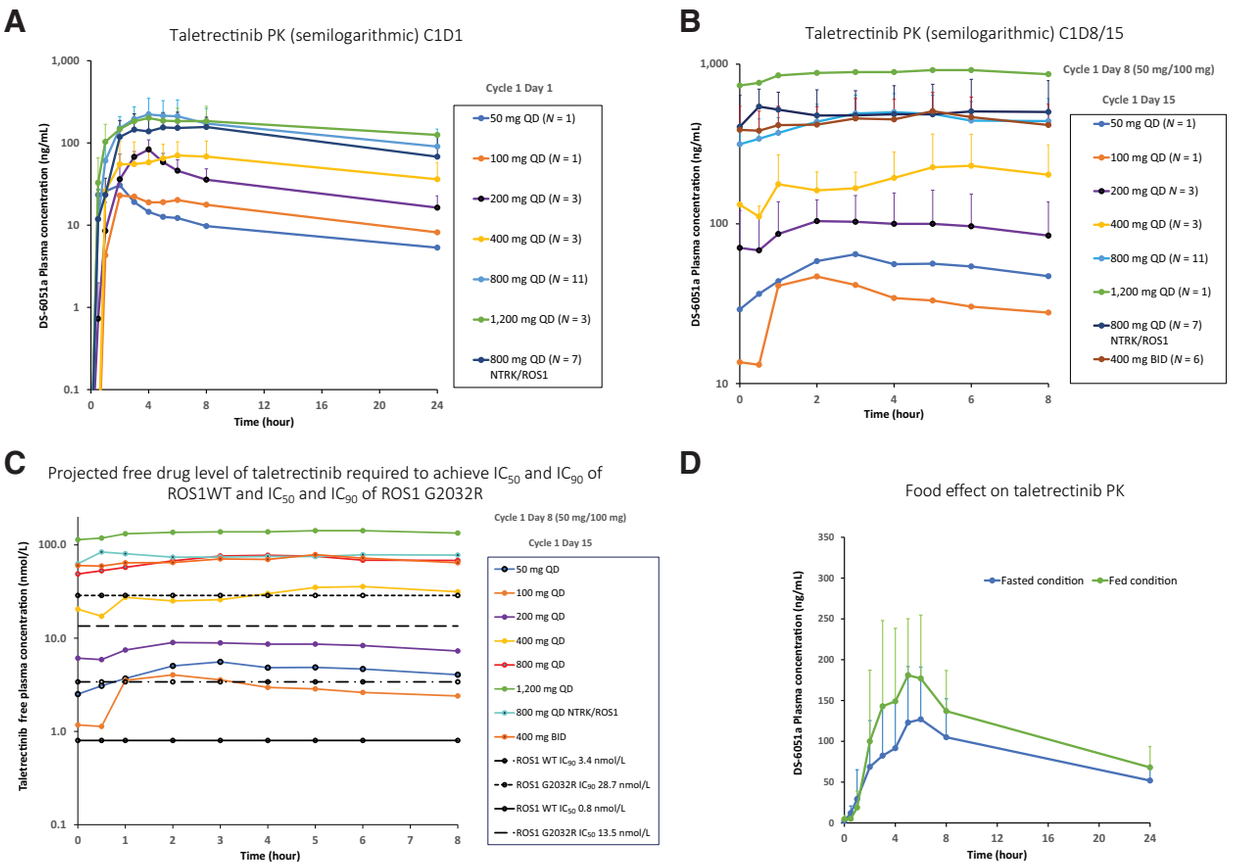

Figure 1.

A, Single-dose PK curves with increasing dose of taletrectinib on cycle 1 day 1 (C1D1). **B,** Steady-state PK curves with increasing dose of taletrectinib on cycle 1 day 15 (C1D8 for 50 mg and 100 mg once daily). **C,** Projected free drug level of taletrectinib required to achieve IC_{50} and IC_{90} of *ROS1* WT and IC_{50} and IC_{90} of *ROS1* G2032R superimposed on the steady-state free drug levels of taletrectinib at various dosing concentration. **D,** Food effect PK curves with taletrectinib.

Food effect

A total of 14 patients were enrolled into the food effect. Eight patients were randomly assigned to the fasted then fed sequence (fasted/fed) while six patients were randomly assigned to the fed then fasted (fed/fasted) sequence. Three patients (one fasted/fed and two fed/fasted) were found to be ineligible. Thus, 11 patients completed the 21-day food effect study [fed/fasted ($N = 4$); fasted/fed ($N = 7$)]. The geometric mean $AUC_{0\text{-}24}$ for the fasted state was 1,810 ng*hour/mL and 2,235 ng*hour/mL for the fed state. The ratio of the geometric mean of $AUC_{0\text{-}24}$ between fed/fasted state was 123% (90% CI, 104%–149%) resulting in a 23% increase from fasted to fed state. The maximum concentration C_{max} was 123.2 ng/mL (fasted) and 178.9 ng/mL (fed). The ratio of the geometric mean of C_{max} between low-fat-diet-fed/fasted was 145% (90% CI, 120%–175%) resulting in a 45% increase from fasted to fed state (**Fig. 1D**). The median T_{max} in the fed state was 5.0 hours compared with 5.92 hours in the fasted state (**Fig. 1D**).

DLTs

MTD was determined to be 800 mg once daily after two of three patients at 1,200 mg once daily developed DLTs. One patient at 1,200 mg once daily dose developed grade 3 syncope, grade 2 AST and ALT elevations which resolved after 14 days of dose interruption (satisfying protocol-defined DLT) and resumed dosing at 800 mg once daily without recurrence of the DLT events. One patient on 1,200 mg once daily developed grade 3 ALT elevations and discontinued treatment after 6 days. In addition, one patient at the 800-mg once-daily dose expansion cohort developed grade 3 hyponatremia that resolved with dose interruptions for 4 days and resumed treatment at 400 mg once daily. Another patient at 400 mg twice daily dose who received prior nivolumab developed grade 3 rash that resolved after dose interruption with dose resumption at 200 mg once daily without further recurrence (see below).

Treatment-emergent adverse events/treatment-related adverse events

Treatment-emergent adverse events (TEAEs) occurred in all 46 (100.0%) patients. The three most common TEAEs were diarrhea (65.2%), nausea (57.1%), and vomiting (37.0%; **Table 2**). TEAEs most commonly associated with TRK (primarily TrkB) inhibition such as dysgeusia, dizziness, and dysesthesia occurred at a total incidence of 26.1%, 17.4%, and 15.2%, respectively with no grade 3 severity among these three AEs (**Table 2**).

Treatment-related AEs (TRAEs) occurred in 40 of 46 (87.0%) patients. The three most common TRAEs were nausea (47.8%), diarrhea (43.5%), and vomiting (32.6%). Grade 3 TRAEs were AST elevation (6.5%), diarrhea (2.2%), and fatigue (2.2%; **Table 2**). Of note, TRAEs related to specific TRK inhibition such as dysgeusia, numbness, and dysesthesia occurred in 23.9%, 15.2%, and 8.7%, respectively, with

Table 2. List of TEAEs ≥15% and TRAE ≥10% (arranged by symptoms and laboratories).

	Total ($N = 46$)	
TEAE, *n* (%)	**All grade**	**≥Grade 3**
Any TEAE	46 (100.0)	31 (67.4)
Symptoms		
Diarrhea	30 (65.2)	4 (8.7)
Nausea	27 (58.7)	1 (2.2)
Vomiting	22 (47.8)	0
Fatigue	17 (37.0)	3 (6.5)
Dehydration	14 (30.4)	0
Dysgeusia	12 (26.1)	0
Abdominal pain	9 (19.6)	3 (6.5)
Appetite decrease	9 (19.6)	1 (2.2)
Dizziness	8 (17.4)	0
Constipation	7 (15.2)	1 (2.2)
Dysesthesia	7 (15.2)	0
Weight loss	7 (15.2)	0
Laboratories		
AST elevation	10 (21.7)	4 (8.7)
Hypokalemia	9 (19.6)	0
Hypophosphatemia	8 (17.4)	4 (8.7)
ALT elevation	7 (15.2)	1 (2.2)

	Total ($N = 46$)	
TRAE, *n* (%)	**All grade**	**≥Grade 3**
Any TEAE	40 (87.0)	12 (26.1)
Symptoms		
Nausea	22 (47.8)	0
Diarrhea	20 (43.5)	1 (2.2)
Vomiting	15 (32.6)	0
Dysgeusia	11 (23.9)	0
Fatigue	8 (17.4)	1 (2.2)
Dysesthesia	7 (15.2)	0
Dehydration	7 (15.2)	0
Dyspepsia	6 (13.0)	0
Appetite decrease	6 (13.0)	0
Myalgia	5 (10.9)	3 (6.5)
Laboratories		
AST elevation	7 (15.2)	3 (6.5)
ALT elevation	7 (15.2)	0

Abbreviations: TEAE, treatment-emergent adverse event; TRAE, treatment-related adverse event.

no grade 3 severity. Of the 46 patients treated, eight (17.4%) required ≥1 dose reduction with all dose reductions due to AEs. No patient had weight gain of >5% due to taletrectinib.

Seven patients received immune checkpoint inhibitors (ICIs) prior to taletrectinib (range, −129 to −50 days). Only one of the seven patients who received single-agent nivolumab developed grade 3 rash which resolved after stopping taletrectinib. The patient received nivolumab for 100 days and stopped 50 days prior to starting taletrectinib. While the rash was attributed to taletrectnib, it is unknown whether it was precipitated by prior ICI use. No other patients developed rash or other common potential immune-related AEs such as interstitial lung disease, pneumonitis colitis, or nephritis were not observed.

Pain assessment

Pain score assessment was collected every week during the dose-escalation cohorts. There was an increase in the mean pain intensity score in patients on 50 mg ($N = 1$) and 100 mg once daily ($N = 1$; Supplementary Fig. S4A and S4B). but then a decrease in the mean pain intensity score among patients who were on the 400 mg once daily ($N = 3$), 800 mg once daily ($N = 9$), and 400 mg twice daily ($N = 6$) cohorts (Supplementary Fig. 4D–SF). There was no change in the mean pain intensity score for patients on the 200 mg once daily ($N = 3$) and 1,200 mg once daily ($N = 2$; Supplementary Fig. 4C and 4G).

Efficacy

Forty-one (89%) of 46 patients were evaluable for response (**Fig. 2A**; Supplementary Fig. S5A and S5B; Supplementary Table S3) including 12 patients with NET (**Fig. 2B**; Supplementary Table S3). There were four patients who achieved confirmed PRs (two patients with *CD74-ROS1*$^+$ NSCLC, one patient with *TPM3-NTRK1*$^+$ thyroid cancer, and one patient with small-bowel NET). The ORR of the 12 patients with NET was 8.3% (95% CI, 1.5–38.4) with one patient with small-bowel NET achieving confirmed PR with a median PFS of 10.2. months (95%CI, 1.2–not reached; Supplementary Fig. S5C and S5D). This patient initially presented with a 1-cm poorly differentiated nonfunctional, octreotide-scan positive small-bowel NET and multifocal hepatic metastases with the largest metastasis at 15 cm in 2003. The patient subsequently received radiofrequency ablation, primary resection, and partial liver resection, drugs targeting PI3/AKT/mTOR, MAPK, and WNT pathways, sandostatin and combination chemotherapy with SD as the best response (Supplementary Fig. S6A). Genomic profiling of the small-bowel NET was unsuccessful due to insufficient available tumor tissue given the long storage time of the archival tumor tissue (diagnosed in 2003 and enrolled onto the current trial in 2014).

Among the six patients with RECIST-evaluable *ROS1*$^+$ NSCLC all of whom had progressed on crizotinib and were treated with either 800 mg once daily, 1,200 mg once daily, or 400 mg twice daily, the confirmed ORR is 33% (95%CI, 9.7–70.0) and median PFS is 4.1 months (95%CI, 0.5–14.2; **Fig. 2C**; Supplementary Fig. S4E and S4F; Supplementary Table S3). One of these two patients had crizotinib- and ceritinib-refractory *ROS1*$^+$ NSCLC who received 1,200 mg once daily of taletrectinib and achieved a confirmed PR of 8 months prior to progression (**Fig. 3A** and **B**). The initial diagnosis of *ROS1* rearrangement is by FISH. Next-generation sequencing using FondationOne CDx (Foundation Medicine Inc) performed on the biopsy of a progressing liver metastasis while on taletrectinib revealed *CD74-ROS1* and a *ROS1* L2086F mutation both at an estimated mean allele frequency (MAF) of approximately 32% (**Fig. 3C**). *ROS1* L2086F is analogous to *ALK* L1256F (**Fig. 3D**) which is susceptible to inhibition by a TKI without an extended L-ring. This patient was subsequently treated with cabozantinib, a type II ROS TKI, with a PR of 13 months (**Fig. 3B** and **E**; ref. 14). Treatment history of the other *CD74-ROS1*$^+$ NSCLC (detected by Foundation One CDx) patient who achieved a confirmed PR was listed in Supplementary Fig. 6B.

Only one patient (metastatic *TPM3-NTRK1*$^+$ papillary thyroid cancer) with an *NTRK* fusion enrolled to the study, who achieved a DOR of 33.4 months at the time of last tumor assessment (September 2019; **Fig. 4**). The treatment history of this *TPM3-NTRK1* patient prior to taletrectinib included thyroidectomy, chemoradiation, radioactive I-131, sorafenib, three phase I trials of targeted and/or ICIs but no prior

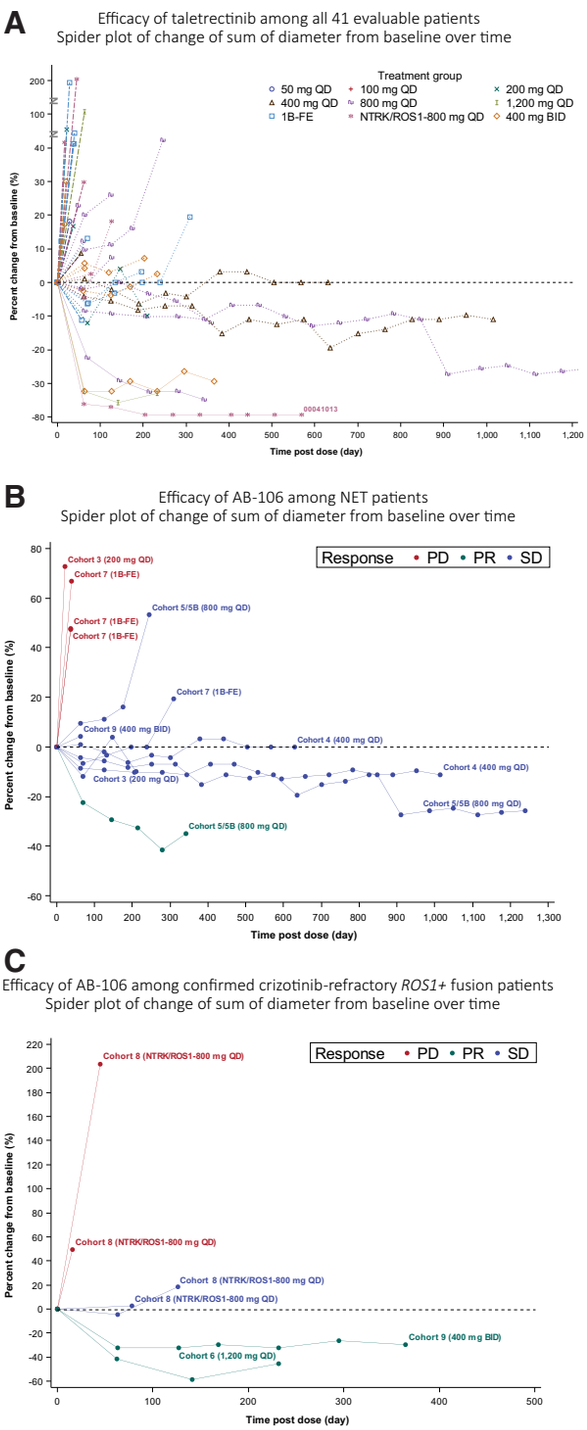

Figure 2.

A, Spider plots of the 41 evaluable patients according to the doses received. **B,** Spider plots of the 12 patients with NET according to the doses received. **C,** Spider plots of the six patients with RECIST-evaluable crizotinib-refractory ROS1$^+$ NSCLC according to the doses received.

NTRK TKIs. The NTRK fusion was detected by Foundation One CDx (Foundation Medicine Inc). Of the two neuroendocrine patients still on treatment at the time data cutoff, one patient has received taletrectinib treatment at 400 mg once daily for 47.2 months and the other patient has been on treatment at 800 mg once daily for 41.4 months (**Fig. 2B**).

Discussion

The MTD of taletrectiib was determined to be 800 mg once daily in this U.S. phase I study. In addition, the food-effect study indicates that a low-fat diet increased the taletrectinib level by 23%. The ratio of geometric mean of $AUC_{0\text{-}24}$ between low-fat-diet-fed/fasted state was 123% (90% CI, 104%–149%) which is outside the range of the 90% CI of 80%–125% considered by the FDA for bioequivalence. Thus, taletectinib is given without food in the current phase II trial of taletrectinib in patients with *ROS1*$^+$ NSCLC in China (ClinicalTrials.gov Identifier: NCT04395677). The projected free plasma taletrectinib at 400 mg once daily is consistently at the IC_{90} necessary to inhibitor *ROS1* G2032R. However, we do note that projected free plasma drug level does not necessary equate to similar intratumoral concentration. The current phase II clinical trial in China will enroll both patients who are TKI-naïve and those with TKI-refractory *ROS1*$^+$ NSCLC.

Side effects of taletrectinib are primarily gastrointestinal in nature (diarrhea, nausea, vomiting) with DLTs being grade 3 liver enzymes elevation at 1,200 mg once daily. Grade 3 TRAEs from taletrectinib are uncommon (<5%) including TRAE-related TrkB inhibition (dysgeusia, dizziness, peripheral neuropathy/numbness; ref. 9). This may be related to the property of taletectinib where it is least potent against TrkB (8). Preliminary clinical efficacy was observed in patients with crizotinib-refractory *ROS1*$^+$ NSCLC with a confirmed ORR of 33% among six evaluable patients. The resistance mechanisms to crizotinib-refractory *ROS1*$^+$ NSCLC were not systemically captured prior to treatment with taletrectinib in this phase I trial. Thus, it is unknown if any of these six patients harbored the *ROS1* G2032R solvent front mutation, the most common acquired resistance mutation to crizotinib (15, 16). In addition, one patient with TKI-naïve *TPM3-NTRK* fusion–positive thyroid cancer achieving an ongoing PFS of 33 months at the time of last follow-up (September 2019; **Fig. 4**).

A smaller phase I study in Japan that enrolled 15 patients with *ROS1*$^+$ NSCLC concluded that the MTD and recommended phase II dose for taletrectinib was 600 mg once daily (17). Two grade 3 ALT elevations were observed at the 800-mg once-daily dose and were considered as DLTs. The steady level of taletrectinib when adjusted by weight is about 32% higher in Japanese patients than in U.S. patients. Diarrhea (53.3%), nausea (46.7%), constipation (33.3%), and creatinine elevation (33.3%) were the most common AEs observed. Among the total of 15 patients with *ROS1*$^+$ NSCLC enrolled, ORR was 66.7% for the nine evaluable patients who were crizotinib-naïve and 33.3% for the three patients with evaluable crizotinib-refractory *ROS1*$^+$. Activity against CNS metastasis was also observed (17). There was no patient with *NTRK* fusion–positive tumors or NET enrolled in the Japanese phase I trial (17).

The elimination half-life of taletrectinib could not be calculated on the basis of this study alone with conventional noncompartmental PK analysis due to insufficient sampling time duration postdose (only 24 hours post the first dose and 8 hours postdose on day 8/15). However, population PK analysis using pooled data from this study and Japan

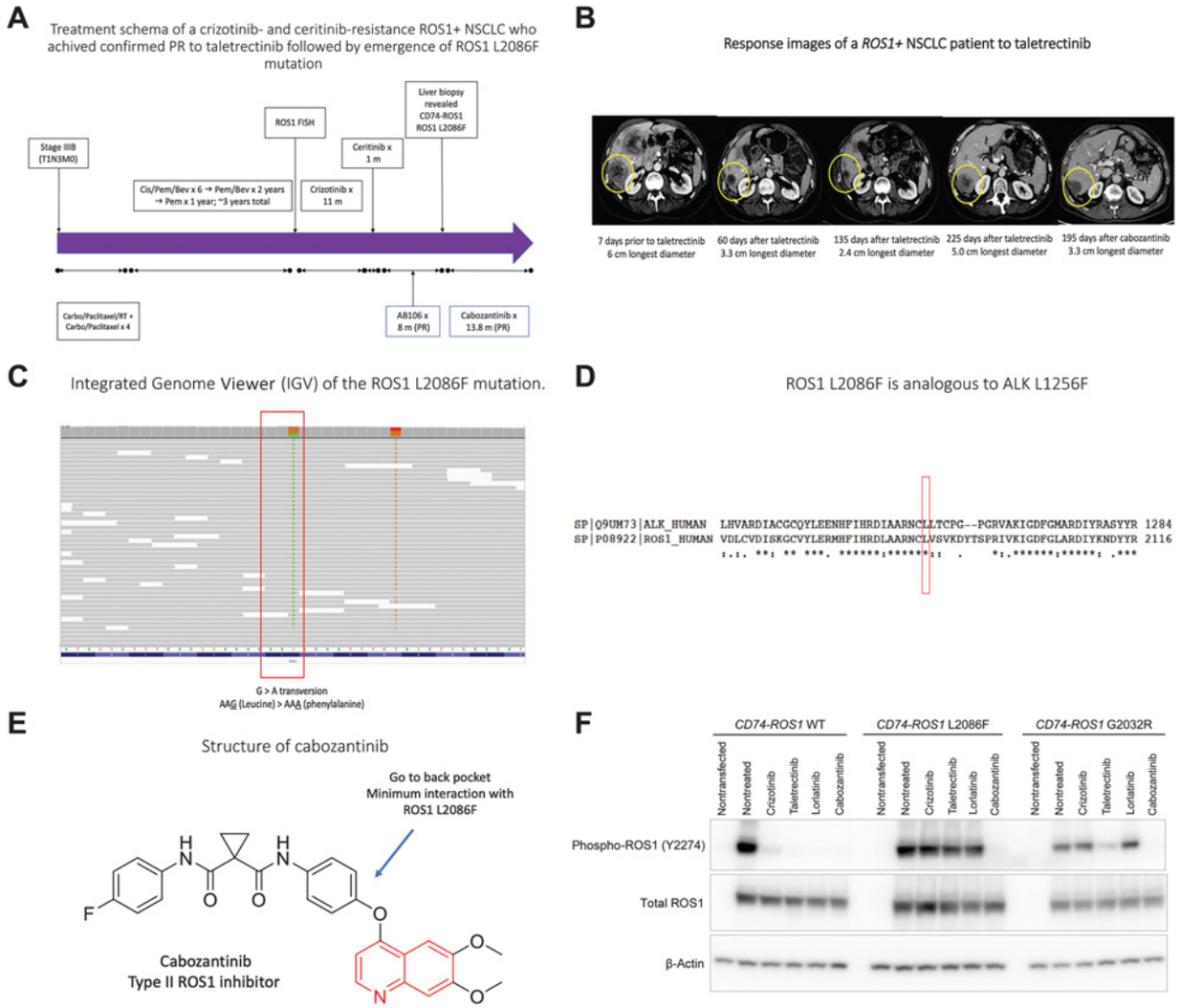

Figure 3.

A, Treatment timeline schema of the ROS1^{+} NSCLC patient who progressed on chemotherapy, crizotinib, ceritinib and achieved a confirmed PR on taletrectinib. NGS on liver biopsy on progression on taletrectinib revealed a ROS1 L2086F. Patient achieved a confirmed PR on cabozantinib. **B,** Response images of the *CD74-ROS1*$^{+}$ NSCLC patient to taletrectinib. **C,** Integrated Genome Viewer (IGV) of the *ROS1* L2086F mutation. MAF of the *ROS1* L2086F is estimated be 32%. Hybrid-capture DNA sequencing indicated *CD74-ROS1* variant at a MAF approximately 32%. **D,** *ROS1* L2086F is analogous to *ALK* L1256F. **E,** Cabozantinib is a type II ROS1 inhibitor which has a large residue passing through the gatekeeper position and extending to the pack pocket and not interfering with F2086. **F,** Cabozantinib and taletrectinib inhibited the phosphorylation of *ROS1* G2032R solvent-front mutation but not crizotinib or lorlatinib. Only cabozantinib inhibited phosphorylation of *ROS1* L2086F mutation but not crizotinib, taletrectinib, or lorlatinib.

phase I data (frequent and sparse PK sampling) indicates the elimination half-life at steady state is about 37.5 hours (geometric mean).

NGF is a ligand to TrkA is involved in pain sensation and strategy to block NTRK pathway has been investigated for pain control (17). Taletrectinib has been shown to be a NTRK inhibitor based on preclinical data and the one patient with NTRK1 fusion–positive thyroid cancer with durable response to taletrectinib. An exploratory analysis in this study revealed stabilization of or modest decrease in the pain intensity score at higher doses of taletrectinib (≥400 mg daily dose). Whether this pain decrease represents pain relief from tumor response or intrinsic pain relief by inhibition of the NTRK pathway remains to be determined.

This is the first report to identify *ROS1* L2086F as a likely on-target resistance mutation to a ROS1 inhibitor. Although we did not perform any comprehensive genomic profiling prior to patient progressing on crizotinib and/or enrollment onto treatment with taletrectinib, several lines of indirect evidence indicate *ROS1* L2086F is an acquired on-target resistance to taletrectinib. First, the MAF of *ROS1* L2086F is relatively high at 32% and at almost identical to the MAF of the *CD74-ROS1* fusion variant indicating *ROS1* L286F was not a minor clone. Second, *ROS1* L2086F is analogous to the *ALK* L1256F mutation (**Fig. 3D**). *ALK* L1256F as a single or as compound mutation has been demonstrated to confer resistance to crizotinib or lorlatinib but sensitive to alectinib

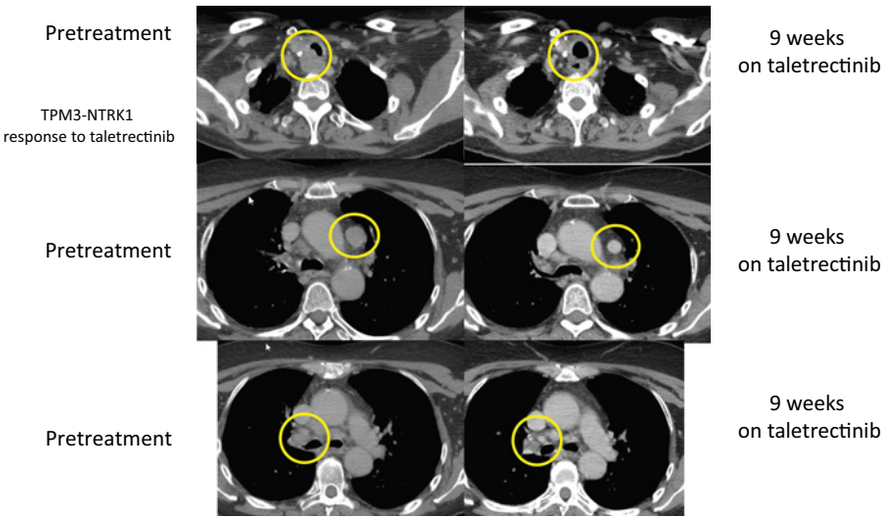

Figure 4.
Tumor response images to taletrectinib in a patient with NTRK TKI-naïve *TPM3-NTRK1* well-differentiated thyroid cancer.

which lacks an L-shape structure (18, 19). Similarly, cabozantinib is a type II ROS1 inhibitor that also lacks an L-shape structure and extends to the pack pocket without stearic interference from a phenylalanine at position 2086 (**Fig. 3E**). Third, *in vitro* experiments demonstrated that cabozantinib but not crizotinib, taletrectinib, or lorlatinib inhibited the phosphorylation of ROS1 L2086F (**Fig. 3F**). Fourth, given our patient achieved a confirmed PR to taletrectinib after progressing on crizotinib and ceritinib, the *ROS1* L2086F mutation detected very likely emerged during treatment with taletrectinib. Consistent with our preclinical data, our patient responded to cabozantinib for >13 months indicated a *ROS1*-dependent resistance mechanism was responsible for the progression on taletrectinib given cabozantinib's documented clinical activity against crizotinib-refractory *ROS1*$^+$ NSCLC (14, 20). Finally, *ROS1* L2086F has recently been shown to be an acquired resistance mutation to lorlatinib (21). Taken all the evidence to date, *ROS1* L2086F is likely on-target resistance mutation to taletrectinib. Our patient case also points to potential sequential use of ROS1 TKIs as depending on the specific on-target resistance mutation. If crizotinib (and entrectinib) is used as the first ROS1 TKI, if and when solvent-front mutation such as *ROS1* G2032R emerges, then potential next ROS1 TKI could be taletrectinib or repotrectinib. When if *ROS1* L2086F emerges as resistance to type I ROS1 TKI, then cabozantinib can be potential considered albeit as off-label use for now.

Currently, crizotinib and entrectinib are the only two ROS1TKIs approved in the United States for treatment of patients with TKI-naïve *ROS1*$^+$ NSCLC (2, 3). Solvent-front mutation *ROS1* G2032R mutation has been well documented as a resistance mechanism to crizotinib (15, 16). In addition, entrectinib is unlikely to overcome the acquired resistance *ROS1* mutations including the most common solvent *ROS1* G2032R solvent-front mutation based on preclinical data (22). *In silico* simulation suggested that docking pose of taletrectinib in ROS1 Gly2032 was almost the same as that in ROS1 WT (Supplementary Fig. S6A and S6B), while crizotinib showed a different docking pose in ROS1 Arg2032 from the binding mode in ROS1 WT (Supplementary Fig. S6C and S6D). Ceritinib, an approved ALK TKI, has demonstrated clinical activity in patients with TKI-naïve *ROS1*$^+$ NSCLC but no clinical activity in those with crizotinib-refractory *ROS1*$^+$ NSCLC (23). Lorlatinib, another ALK/ROS1 TKI, has demonstrated clinical activity in patients with crizotinib-refractory *ROS1*$^+$ NSCLC with an ORR of 35% and median PFS of 8.5 months (24). However, of the six patients with *ROS1* G2032R solvent-front mutation (two *de novo* and four acquired) in the lorlatinib study, the ORR to lorlatinib was 0% consistent with limited preclinical activity (cellular IC_{50} = 203 nmol/L) of lorlatinib against *ROS1* G2032R mutation (24, 25). Furthermore, in the two patients who developed acquired *ROS1* L2026M gatekeeper resistance mutation, the ORR to lorlatinib was also 0% (23). Brigatinib, an ALK TKI, has reported clinical activity in one patient with ceritinib-refractory *ROS1*$^+$ NSCLC (26). Repotrectinib, a next-generation ROS1/NTRK inhibitor, has demonstrated preliminary clinical activity against patients with crizotinib-refractory *ROS1*$^+$ NSCLC (22, 27).

In this phase I study, taletrectinib has demonstrated good safety profile with long-term tolerability as some of the responding patients have been on taletrectinib for a prolonged period (**Fig. 2A–C**), once- a -day dosing convenience, and preliminary confirmed clinical activity in patients with crizotinib-refractory *ROS1*$^+$ NSCLC for whom there is currently no approved next-generation ROS1 TKI (**Fig. 2C**). Currently, one large-scale phase II clinical trials investigating the clinical efficacy of taletrectinib in patients with TKI-naïve and TKI-refractory *ROS1*$^+$ NSCLC is ongoing in China (ClinicalTrials.gov Identifier: NCT04395677). In addition, a phase II trial will commence in Japan soon.

Disclosure of Potential Conflicts of Interest

A.T. Shaw reports grants and personal fees from Novartis (employee, equity), Pfizer, and TP Therapeutics, as well as personal fees from Daiichi-Sankyo (consulting) and Loxo outside the submitted work. R. Katayama reports grants from AMED and Daiichi-Sankyo during the conduct of the study; grants from Chugai, Takeda, and TOPPAN Printing as well as personal fees from Pfizer (speakers bureau honoraria) outside the submitted work. V.W. Zhu reports other from AstraZeneca (consulting, speaker program), Roche-Foundation Medicine (speaker program), Roche/Genentech (consulting, speaker program), and TP Therapeutics (prior stock ownership) outside the submitted work. H.A. Wakelee reports personal fees from Daiichi-Sankyo (single advisory board) during the conduct of the study; personal fees from AstraZeneca (single advisory board, clinical trial support), Mirati (advisory board), Helsinn (advisory board), and Blueprint (advisory board), as well as Arrys Therapeutics (clinical support to institution), Bristol-Myers Squibb (clinical support to institution), Exelixis (clinical support to institution), Genentech/Roche (clinical support to institution), Merck (clinical support to institution), Novartis (clinical support to

institution), and Xcovery (clinical support to institution) outside the submitted work. R. Madison reports personal fees from Foundation Medicine (Employment) and Roche (Stock) outside the submitted work. A. B. Schrock reports personal fees from Foundation Medicine (employment, a wholly owned subsidiary of Roche) and other from Roche (stock ownership) during the conduct of the study. G. Senaldi is an employee of Daiichi Sankyo. N. Nakao is an employee of Daiichi Sankyo. T. Masaya is an employee of Daiichi Sankyo. T. Isoyama is an employee of Daiichi Sankyo. M. Li reports personal fees from AnHeart Therapeutics (Hangzhou) Company Ltd (employee) outside the submitted work. T. Seto reports grants from Daiichi Sankyo during the conduct of the study; reports grants and personal fees from AstraZeneca (honoraria), Chugai Pharmaceutical (honoraria), Daiichi Sankyo (honoraria), Eli Lilly Japan (honoraria), MSD (honoraria), Nippon Boehringer Ingelheim (honoraria), Novartis Pharma (honoraria), Takeda Pharmaceutical (honoraria), and Pfizer Japan (honoraria); reports personal fees from Astellas Pharma (honoraria), Bristol-Myers Squibb (honoraria), Kyowa Hakko Kirin (honoraria), Ono Pharmaceutical (honoraria), Taiho Pharmaceutical (honoraria), Thermo Fisher Scientific (honoraria), and Precision Medicine Asia (employment); and reports grants from Abbvie, Bayer Yakuhin, Kissei Pharmaceutical, LOXO Oncology, and Merck Biopharma outside the submitted work. P.A. Janne reports grants and personal fees from Daiichi Sankyo and personal fees from Pfizer, Roche/Genentech, and Ignyta during the conduct of the study; reports grants and personal fees from AstraZeneca, Boehringer Ingelheim, Eli Lilly, and Takeda Oncology; reports personal fees from ACEA Biosciences, LOXO Oncology, Araxes Pharmaceuticals, SFJ Pharmaceuticals, Voronoi, Biocartis, Novartis, and Sanofi; and reports grants from Astellas and Revolution Medicines outside the submitted work, as well as a patent regarding EGFR mutations owned by DFCI and licensed to Lab Corp. S.I. Ou reports grants from Daiichi Sankyo (institution grant for the research done) during the conduct of the study; reports personal fees from Pfizer (consulting fee, speakers bureau), AstraZeneca (consulting fee, speakers bureau), Daiichi Sankyo (consulting fees), Roche/Genentech (consulting fees, speakers bureau), Takeda/ARIAD (consulting fees, speaker fees), Spectrum Pharmaceuticals (consulting fees), and Merck (speakers bureau), as well as other from Turning Point Therapeutics (stock ownership, previous member of scientific advisory board) outside the submitted work.

Authors' Contributions

K.P. Papadopoulos: Data curation, funding acquisition, investigation, writing-review and editing. **E. Borazanci:** Data curation, investigation, writing-review and editing. **A.T. Shaw:** Data curation, investigation, writing-review and editing. **R. Katayama:** Data curation, investigation, writing-review and editing. **Y. Shimizu:** Data curation, methodology, writing-review and editing. **V.W. Zhu:** Data curation, writing-review and editing. **T.Y. Sun:** Data curation, writing-review and editing. **H.A. Wakelee:** Data curation, writing-review and editing. **R. Madison:** Data curation, writing-review and editing. **A.B. Schrock:** Investigation, writing-review and editing. **G. Senaldi:** Data curation, investigation, writing-review and editing. **N. Nakao:** Data curation, formal analysis, methodology, writing-review and editing. **H. Hanzawa:** Data curation, writing-review and editing. **M. Tachibana:** Conceptualization, resources, data curation, formal analysis, supervision, funding acquisition, investigation, methodology, project administration, writing-review and editing. **T. Isoyama:** Data curation, software, methodology, writing-review and editing. **K. Nakamaru:** Conceptualization, supervision, funding acquisition, writing-review and editing. **C. Deng:** Data curation, methodology, writing-review and editing. **M. Li:** Data curation, software, formal analysis, writing-review and editing. **F. Fran:** Resources, data curation, project administration, writing-review and editing. **Q. Zhao:** Data curation, formal analysis, validation, methodology, writing-review and editing. **Y. Gao:** Data curation, software, formal analysis, writing-review and editing. **T. Seto:** Investigation, writing-review and editing. **P.A. Jänne:** Data curation, formal analysis, investigation, writing-review and editing. **S.-H.I. Ou:** Data curation, formal analysis, funding acquisition, investigation, methodology, writing-original draft, writing-review and editing.

Acknowledgments

This trial is supported by Daiichi Sankyo, Inc and AnHeart Therapeutics Company.

We thank Xuemin Gu from Daiichi Sankyo, USA for the statistical help, Jon Greenberg from Daiichi Sankyo, USA for continual clinical support of the trial for the 3 patients still on study after data cutoff. The study is funded by Daiichi Sankyo, USA and AnHeart Therapeutics Inc, Hangzhou, China.

The costs of publication of this article were defrayed in part by the payment of page charges. This article must therefore be hereby marked *advertisement* in accordance with 18 U.S.C. Section 1734 solely to indicate this fact.

Received April 28, 2020; revised June 6, 2020; accepted June 24, 2020; published first June 26, 2020.

References

1. Schram AM, Chang MT, Jonsson P, Drilon A. Fusions in solid tumours: diagnostic strategies, targeted therapy, and acquired resistance. Nat Rev Clin Oncol 2017;14:735–48.
2. Shaw AT, Ou SH, Bang Y-J, Camidge DR, Slomon BJ, Salgia R, et al. Crizotinib in ROS1-rearranged non small-cell lung cancer. N Engl J Med 2014;371:1963–71.
3. Drilon A, Siena S, Dziadziuszko R, Barlesi F, Krebs MG, Shaw AT, et al. Entrectinib in *ROS1* fusion-positive non-small-cell lung cancer: integrated analysis of three phase 1–2 trials. Lancet Oncol 2020;21:261–70.
4. Drilon A, Laetsch TW, Kummar S, DuBois SG, Lassen UN, Demetri GD, et al. Efficacy of larotrectinib in TRK fusion-positive cancers in adults and children. N Engl J Med 2018;378:731–39.
5. Doebele R, Drilon A, Paz-Ares L, Siena S, Shaw AT, Farago A, et al. Entrectinib in patients with advanced or metastatic NTRK fusion-positive solid tumours: integrated analysis of three phase 1–2 trials. Lancet Oncol 2020;21:271–82.
6. Osborne JK, Larsen JE, Gonzales JX, Shames DS, Sato M, Wistuba II, et al. NeuroD1 regulation of migration accompanies the differential sensitivity of neuroendocrine carcinomas to TrkB inhibition. Oncogenesis 2013;2:e63.
7. Chang DS, Hsu E, Hottinger DG, Cohen SP. Anti-nerve growth factor in pain management: current evidence. J Pain Res 2016;9:373–83.
8. Katayama R, Gong B, Togashi N, Miyamoto M, Kiga M, Iwasaki S, et al. The new-generation selective ROS1/NTRK inhibitor DS-6051b overcomes crizotinib resistant ROS1-G2032R mutation in preclinical models. Nat Commun 2019; 10:3604.
9. Cocco E, Scaltriti M, Drilon A. NTRK fusion-positive cancers and TRK inhibitor therapy. Nat Rev Clin Oncol 2018;15:731–47.
10. O'Quigley J, Pepe M, Fisher L. Continual reassessment method: a practical design for phase 1 clinical trials in cancer. Biometrics 1990;46:33–48.
11. O'Quigley J, Shen LZ. Continual reassessment method: a likelihood approach. Biometrics 1996;52:673–84.
12. Fishman B, Pasternak S, Wallenstein SL, Houde RW, Holland JC, Foley KM. The memorial pain assessment card. A valid instrument for the evaluation of cancer pain. Cancer 1987;60:1151–8.
13. Wilson EB. Probable inference, the law of succession, and statistical inference. J Am Stat Assoc 1927;22:209–12.
14. Sun TY, Niu X, Chakraborty A, Neal JW, Wakelee HA. Lengthy progression-free survival and intracranial activity of cabozantinib in patients with crizotinib and ceritinib-resistant ROS1-positive non-small cell lung cancer. J Thorac Oncol 2019;14:e21–4.
15. Gainor JF, Tseng D, Yoda S, Dagogo-Jack I, Friboulet L, Lin JJ, et al. Patterns of metastatic spread and mechanisms of resistance to crizotinib in ROS1-positive non-small-cell lung cancer. JCO Precis Oncol 2017;2017. DOI: 10.1200/PO.17.00063. Published online August 1, 2017.
16. Dagogo-Jack I, Rooney M, Nagy RJ, Lin JJ, Chin E, Ferris LA, et al. Molecular analysis of plasma from patients with ROS1-positive non-small cell lung cancer. J Thorac Oncol 2019;14:816–24.
17. Fujiwara Y, Takeda M, Yamamoto N, Nakagawa K, Nosaki K, Toyozawa R, et al. Safety and pharmacokinetics of DS-6051b in Japanese patients with non-small cell lung cancer harboring ROS1 fusions: a phase I study. Oncotarget 2019;9: 23729–37.
18. Gainor JF, Dardaei L, Yoda S, Friboulet L, Leshchiner I, Katayama R, et al. Molecular mechanisms of resistance to first- and second-generation ALK inhibitors in ALK-rearranged lung cancer. Cancer Discov 2016;6: 1118–33.

19. Yoda S, Lin JJ, Lawrence MS, Burke BJ, Friboulet L, Langenbucher A, et al. Sequential ALK inhibitors can select for lorlatinib-resistant compound ALK mutations in ALK-positive lung cancer. Cancer Discov 2018;8:714–29.
20. Drilon A, Somwar R, Wagner JP, Vellore NA, Eide CA, Zabriskie MS, et al. A novel crizotinib-resistant solvent-front mutation responsive to cabozantinib therapy in a patient with ROS1-rearranged lung cancer. Clin Cancer Res 2016;22:2351–8.
21. Lin JJ, Johnson T, Lennerz JK, Lee C, Hubbeling HG, Yeap BY, et al. Resistance to lorlatinib in *ROS1* fusion-positive non-small cell lung cancer. J Clin Oncol 38:15s, 2020 (suppl; abstr 9611).
22. Drilon A, Ou SI, Cho BC, Kim DW, Lee J, Lin JJ, et al. Repotrectinib (TPX-0005) is a next-generation ROS1/TRK/ALK inhibitor that potently inhibits ROS1/TRK/ALK solvent- front mutations. Cancer Discov 2018;8:1227–36.
23. Lim SM, Kim HR, Lee JS, Lee KH, Lee YG, Min YJ, et al. Open-label, multicenter, phase II study of ceritinib in patients with non-small-cell lung cancer harboring ROS1 rearrangement. J Clin Oncol 2017;35:2613–8.
24. Shaw AT, Solomon BJ, Chiari R, Riely J, Besse B, Soo RA, et al. Lorlatinib in advanced ROS1-positive non-small-cell lung cancer: a multicentre, open-label, single-arm, phase 1–2 trial. Lancet Oncol 2019;20:1691–1701.
25. Zou HY, Li Q, Engstrom LD, West M, Appleman V, Wong KA, et al. PF-06463922 is a potent and selective next-generation ROS1/ALK inhibitor capable of blocking crizotinib-resistant ROS1 mutations. Proc Natl Acad Sci U S A. 2015;112:3493–8.
26. Hegde A, Hong DS, Behrang A, Ali SM, Juckett L, Meric-Bernstam F, et al. Activity of brigatinib in crizotinib and ceritinib-resistant ROS1-rearranged non–small-cell lung cancer. JCO Precis Oncol 2019. Published online February 15, 2019. https://doi.org/10.1200/PO.18.00267
27. Cho BC, Drilon AE, Doebele RC, Kim DW, Lin JJ, Lee J, et al. Safety and preliminary clinical activity of repotrectinib in patients with advanced ROS1 fusion-positive non-small cell lung cancer (TRIDENT-1 study). J Clin Oncol 37:15s, 2019(suppl; abstr 9011).